Technical note: Benchmark time-temperature paths provide a shared framework for evaluating and communicating thermochronologic data interpretation

Andrea L. Stevens Goddard[1], Kendra E. Murray[2], Alyssa A. Abbey[3], and Mark Wildman[4]

[1]Department of Earth and Atmospheric Sciences, Indiana University, 1001 E 10th St., Bloomington, IN 47408, USA
[2]Department of Geosciences, Idaho State University, 921 South 8th Avenue, Pocatello, ID 83209, USA
[3]Department of Geological Sciences, California State University, Long Beach, 1250 Bellflower Boulevard, Long Beach, CA 90840, USA
[4]School of Geographical and Earth Sciences, University of Glasgow, 8NN, University Ave, Glasgow, UK

Technical note: Benchmark time-temperature paths provide a shared framework for evaluating and communicating thermochronologic data interpretation

Andrea L. Stevens Goddard[1], Kendra E. Murray[2], Alyssa A. Abbey[3], and Mark Wildman[4]

[1]Department of Earth and Atmospheric Sciences, Indiana University, 1001 E 10th St., Bloomington, IN 47408, USA
[2]Department of Geosciences, Idaho State University, 921 South 8th Avenue, Pocatello, ID 83209, USA
[3]Department of Geological Sciences, California State University, Long Beach, 1250 Bellflower Boulevard, Long Beach, CA 90840, USA
[4]School of Geographical and Earth Sciences, University of Glasgow, 8NN, University Ave, Glasgow, UK

1. Abstract

We present a set of six time-temperature (tT) histories, which we refer to as benchmark paths, that can be used as a shared framework for evaluating the sensitivity of a thermochronologic system to the variables inherent in the interpretation of thermochronologic data (e.g., kinetics models, mineral compositions or geometries, etc.). These benchmark paths span 100 Myr, include monotonic and nonmonotonic histories that represent plausible geologic scenarios, and have a range of cooling rates through different chronometer partial retention/annealing temperatures. Here, we demonstrate their utility by presenting a method for "tuning" these paths to 11 different kinetics models for the apatite (U-Th-Sm)/He (n=5), apatite fission-track (n=2), and zircon (U-Th)/He (n=4) systems. These tuned tT paths provide a practical comparison of the kinetics models for each system and the data patterns they predict, thereby offering anyone performing thermal history analysis the ability to consider how their choice of kinetics model may impact their data interpretation. The adoption of benchmark paths for evaluating kinetics models and other variables provides a practical way to evaluate and communicate the decision-making processes that are inherent in thermochronologic modeling and data interpretation.

2. Introduction

We propose adopting a common set of thermal (time-temperature, *tT*) histories, called benchmark paths, for the apatite (U-Th-Sm)/He, apatite fission-track, and zircon (U-Th)/He systems (hereafter AHe, AFT, and ZHe, respectively). These benchmark paths can be used for a variety of applications because they are designed to highlight the sensitivity of each thermochronometric system to differences in kinetics models, tT history features, mineral compositions/geometries, and other variables critical to the interpretation of thermochronologic data. For example, here we demonstrate the utility of these benchmark paths by using them to visualize and quantify the consequences of choosing different kinetics models to interpret cooling ages.

3. Designing the benchmark thermal histories

Figure 1 presents a general representation of our proposed benchmark paths, which are inspired by the paths in Wolf et al. (1998) and designed with the following criteria. Together, these paths:

1. include simulations of both monotonic and non-monotonic thermal histories
2. explore a range of cooling rates through a chronometer's closure temperature window
3. represent geologically plausible thermal histories

The proposed 100-Myr-long benchmark paths represent distinct but realistic geologic histories that capture simple monotonic cooling (Paths 1, 2) and complete thermal resetting (Path 6), in addition to complex thermal conditions such as sustained residence in the closure temperature window (Paths 3, 4) and reheating that results in partial resetting (Path 5) that tend to produce more complicated data sets.

Each of the six proposed benchmark thermal histories are representative of a geologic setting in the following ways. Path 1 simulates rapid cooling, like that associated with post-eruptive cooling of a volcanic rock. Path 2 represents protracted cooling, typical of cratonic erosion. Path 3 represents rapid rock cooling, such as is associated with rift initiation settings. Path 4 shows cooling representative of erosion patterns in emerging topography, like that in an active thrust belt. Path 5 includes heating at rates typical of basin burial followed by cooling associated with basin inversion and exhumation. Path 6 simulates transient localized heating and cooling, similar to what may happen next to a near-surface igneous intrusion. Each of these geologic scenarios has a different duration and rate of cooling through the closure temperature window (Fig. 1).

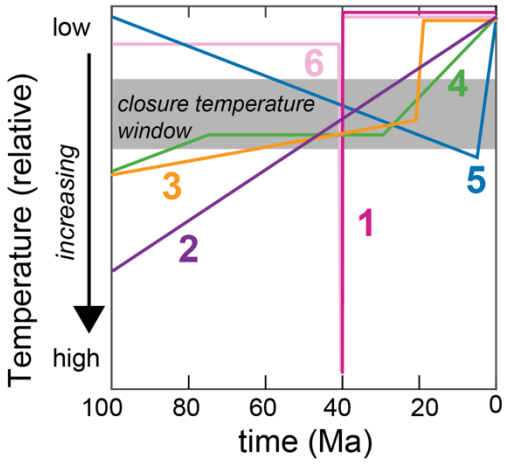

Figure 1. Proposed benchmark paths with relative temperature histories. Paths 1-5 are inspired by the Wolf et al. (1998) demonstration of the non-uniqueness of a single cooling age and were modified by Murray et al. (2022).

In this contribution, we decided to tune these paths such that they all predict a 40 Ma age for a specific grain composition and/or size because this facilitates an inverse approach. In other words, we visualize the results as the range of tT paths that are all tuned to produce a 40 Ma age, where the tuned differences in the tT paths reflect the consequences of the thermal history model inputs (e.g., kinetics model, etching protocols, grain geometry, mineral chemistry). This mimics the most common thermochronologic workflow, where cooling age(s) are measured and tT modeling is used to find the range of tT histories that fit those data. Designing each benchmark path to produce a single 40 Ma age also means that they inherently demonstrate the nonuniqueness of individual cooling ages (Wolf et al., 1998). Thus, for thermochronologists

already proficient in the differences among the kinetics models, our tuning method and results provide a simple quantitative demonstration of expected chronometer behaviors that can be further tuned for new kinetics models or different geological scenarios; for others, this contribution can provide an on-ramp to building such expertise.

4. Tuning benchmark paths to specific kinetics models

We demonstrate the utility of the proposed benchmark paths by using them to illustrate the different temperature sensitivities of three low-temperature thermochronometers (AHe, AFT, ZHe), and then, within each system, how kinetics models also require different temperatures to produce the same age. This is useful because although experimentally derived kinetics models provide the foundation for the interpretation of thermochronologic data, it can be difficult to develop a practical understanding of if or how choosing one kinetics model over another might impact one's thermal history model results. This is critical for both project design and data interpretation.

Most publications that introduce new kinetics models use example tT histories that are calibrated to demonstrate the nuances of that specific kinetics model, in addition to the mathematical calibrations that include intrinsic mineral features including chemistry, radiogenic element concentration, and geometries (e.g., Wolf et al., 1996; Carlson et al., 1999; Donelick et al., 1999; Ketcham et al., 1999; Farley, 2000; Reiners et al., 2004; Flowers et al., 2009; Gautheron et al., 2009; Guenthner et al., 2013; Willett et al., 2017; Ginster et al., 2019; Guenthner, 2021). For example, Flowers et al. (2009) demonstrated the RDAAM AHe kinetics model using the ~300 Myr history of the Esplanade Sandstone and the ~1800 Myr history of basement samples from the Canadian Shield. The α-recoil damage AHe kinetics model was introduced by Gautheron et al. (2009) using the ~300 Myr duration geologic history of the French Massif Central. Willet et al. (2017) uses the predicted ages from a ~550 Myr duration geologic history from the Grand Canyon to present the ADAM AHe kinetics model. These individualized tT histories remain a fundamental contribution because they demonstrated behaviors distinctive to a particular kinetics model and the rocks these models were first applied to. Our benchmark paths complement these contributions by providing a universal reference frame that can be used to compare these kinetics models.

Each of the benchmark paths are tuned to produce a 40 Ma age in crystals with the following standard sizes and compositions. For the AHe system, the crystal is assigned a spherical radius (Rs) of 60 μm and a U concentration of 60 ppm. For the AFT system, we use a Dpar = 2.05 μm for grains etched in 5.5M HNO_3 for 20 seconds (Sobel & Seward, 2010). For the ZHe system, we use a crystal with Rs = 60 μm and [U] = 600 ppm.

To tune a general benchmark path (Fig. 1) to a specific thermochronometer and an associated kinetics model, we held constant the timing of heating and cooling events but modified the maximum temperatures that control the timing and duration of passage through the system's closure temperature window to produce a 40 Ma age (Fig. 2, Table 1). Practically, this requires changing the temperature of one node of the tT path for each kinetics model (Fig. 2, Table 1).

Additionally, for each system (AHe, AFT, ZHe), benchmark paths 3 and 4 are assigned an initial temperature at 100 Ma that is necessary for simulating slow cooling or isothermal holding within the chronometer's closure temperature window (Fig. 2, Table 1). Then, we further tuned the benchmark paths for each chronometer to all produce a 40 Ma age using the following specific kinetics models:(1) the AHe system including Wolf et al. (1998), Farley (2000), Flowers et al., (2009), Gautheron et al. (2009), and Willett et al., (2017); (2) the AFT system including Ketcham et al., (1999) and Ketcham et al. (2007); and (3) the ZHe system including Reiners et al., (2004), Guenthner et al. (2013), Ginster et al. (2019), and Guenthner (2021) implementation of the ZRDAAM without annealing (Fig. 2, Table 1).

	kinetics model citation		Path 1			Path 2		Path 3				Path 4				Path 5			Path 6				
		time (Ma)	*40*	*39.9*	*0*	*100*	*0*	*100*	*21*	*19*	*0*	*100*	*75*	*30*	*0*	*100*	*5*	*0*	*100*	*41*	*40.5*	*40*	*0*
apatite (U-Th)/He	*Wolf et al., 1996*	T (°C)	200	5	5	150	5	90	51	5	5	90	62	62	5	5	64	5	20	20	200	5	5
	Farley, 2000	T (°C)	200	5	5	130	5	90	42	5	5	90	54	54	5	5	57	5	20	20	200	5	5
	Flowers et al., 2009	T (°C)	200	5	5	145	5	90	61	5	5	90	71	71	5	5	83	5	20	20	200	5	5
	Gautheron et al., 2009	T (°C)	200	5	5	185	5	90	76	5	5	90	82	82	5	5	90	5	20	20	200	5	5
	Willett et al., 2017	T (°C)	200	5	5	150	5	90	65	5	5	90	73	73	5	5	83	5	20	20	200	5	5
AFT*	*Ketcham et al., 2007*	T (°C)	200	5	5	230	5	130	81	5	5	120	93	93	5	5	99	5	20	20	200	5	5
	Ketcham et al., 1999	T (°C)	200	5	5	255	5	130	96	5	5	120	105	105	5	5	111	5	20	20	200	5	5
zircon (U-Th)/He	*Reiners et al., 2004*	T (°C)	200	5	5	440	5	240	149	5	5	300	172	172	5	5	180	5	20	20	260	5	5
	Guenthner et al. 2013	T (°C)	200	5	5	400	5	240	140	5	5	300	164	164	5	5	181	5	20	20	260	5	5
	Guenthner, 2021	T (°C)	200	5	5	435	5	240	145	5	5	300	168	168	5	5	182	5	20	20	260	5	5
	Ginster et al., 2019	T (°C)	200	5	5	421	5	240	141	5	5	300	165	165	5	5	180	5	20	20	260	5	5

change Temperature across chronometer

change Temperature across kinetics model

*Apatite Fission Track (AFT)

Table 1. Benchmark Paths tuned to produce a 40 Ma cooling age for common legacy and modern kinetics models for the apatite (U-Th)/He, apatite fission track, and zircon (U-Th)/He systems.

Within each chronometric system, this exercise provides a sensitivity test of kinetics models. For example, for the AHe, AFT, and ZHe systems, the same temperature conditions predict the same cooling age for rapid cooling associated with igneous processes (Fig. 2, Paths 1, 6). This suggests that the choice of a kinetics model in these thermal conditions will not change the interpretation of the data, as has been previously discussed in the papers that originally presented these kinetics models (e.g., Ketcham et al., 1999; Flowers et al., 2009; Guenthner et al., 2013).

By contrast, paths that feature slow cooling or prolonged residence at and/or reheating to partial retention/annealing temperatures require different temperatures to predict the same cooling age; making the corollary also true: measured cooling age(s) may fit different cooling histories if using different kinetics models (Fig. 2). For example, the thermal histories that produce a Path 4, 40 Ma cooling age for the AHe system require that the crystals are held at temperatures between 75 and 29.5 Ma, but the difference in this holding temperature can vary by nearly 30°C depending on the kinetics model used (Fig. 2). This variability in holding temperatures is much lower, ~ 10°C, for the AHe kinetics models that incorporate the effects of radiation damage and annealing (Flowers et al., 2009; Gautheron et al., 2009; Willett et al., 2017) but could still modify the geologic interpretations of such a data set. Interpretations using kinetics from a legacy AHe kinetics model that does not consider the effects of radiation damage and annealing (e.g., Wolf et al., 1996; Farley, 2000) should be reevaluated. For the AFT system, Path 4 benchmark

thermal histories also vary. The legacy kinetics model of Ketcham (1999) requires a retention temperature ~ 10°C higher than the kinetics model of Ketcham et al. (2007). By contrast, Path 4 benchmark thermal histories for ZHe kinetics models from Guenthner et al. (2013) and Ginster et al., (2019) differ by only ~ 1°C indicating that the choice of one kinetics model over the other will not modify the interpretation of such a data set.

We propose that for any new kinetics model, a new tuned set of benchmark paths is made that can be compared with those tuned to existing kinetics models (Fig. 2). This set of benchmark paths would be tuned by modifying the maximum temperature within the closure temperature window of each mineral system to generate a predicted cooling age of 40 Ma ± 1 Ma using a particular kinetics model (Fig. 2, Table 1).

5. Using benchmark paths to visualize the additional effects of compositional variations in datasets with more than one analysis

Once tuned, each benchmark tT path can be used in a forward sense to predict He ages for other crystal sizes and [U] compositions (e.g., age-[eU]

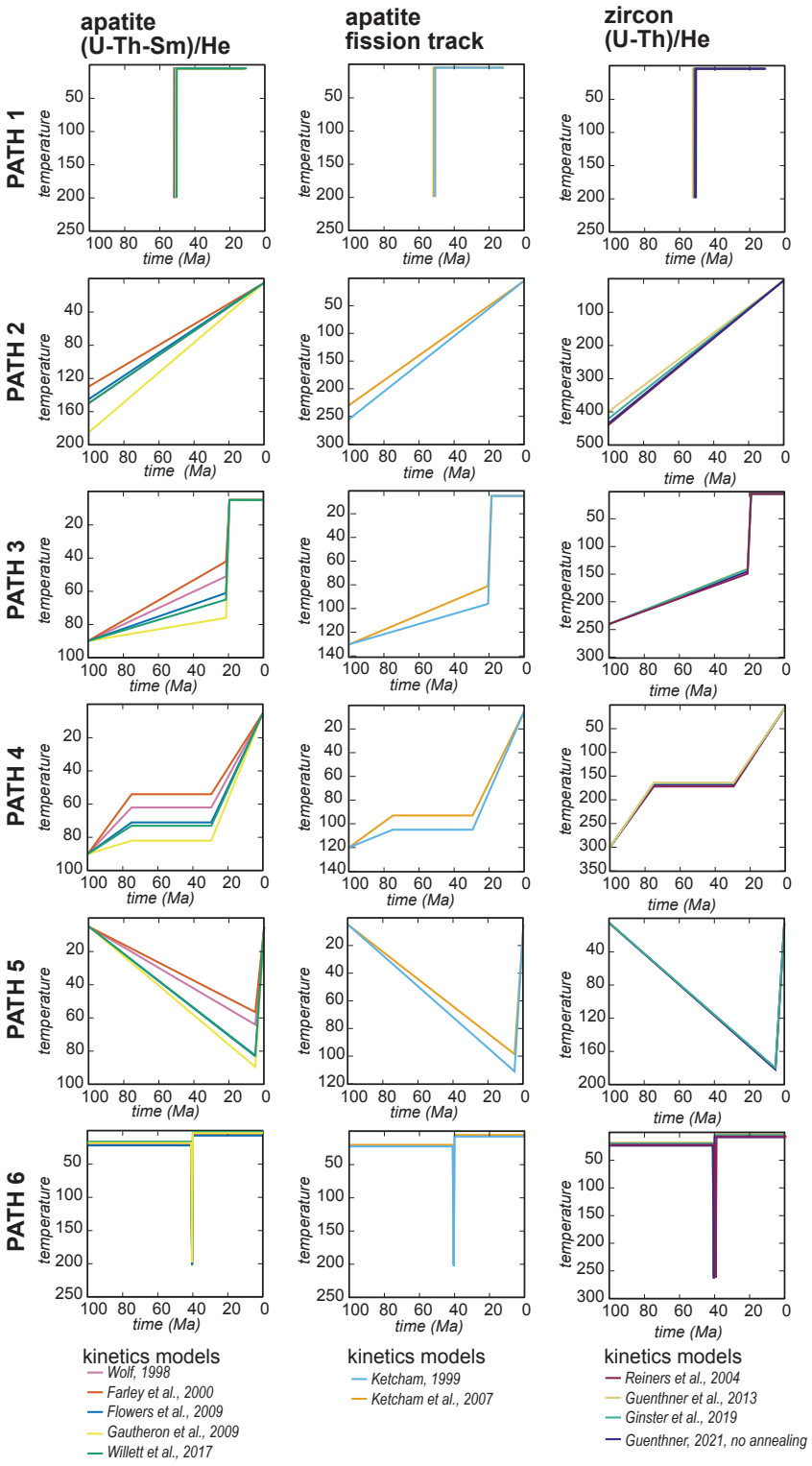

Figure 2. Benchmark paths shown in tT space. Benchmark paths are tuned to produce a 40 Ma cooling age using published legacy and modern kinetics models of the AHe, AFT, and ZHe systems.

trends; effective U, [eU] = [U] + 0.234*[Th] + 0.0047*[Sm]) and AFT track-length distributions (Fig. 3). Expanding the predicted results of a benchmark path in these ways simulates the resolving power of a real dataset with multiple analyses and demonstrates how the choice of kinetics model may impact the possible fits to the data.

For the AHe and ZHe systems, we used tuned benchmark paths to predict multiple He ages from a range of crystal [eU] compositions and thereby quantify and visualize the potential impact of choosing one kinetics model over another during data analysis (Fig. 3). Simple and fast cooling, like Paths 1 and 6, or steady and monotonic cooling, like Path 2, produce minimal differences in the data patterns predicted by different kinetics models (Fig. 3). For example, Paths 1 and 6 predict AHe cooling ages with a difference of ~1 Myr using the three published kinetics models that account for radiation damage accumulation and annealing effects (Flowers et al. 2009; Gautheron et al.,2009, Willett et al 2017) for crystals with [eU] values ranging from 10 ppm to 300 ppm. For the same [eU] apatite crystals, Path 2 predicts cooling ages that differ by between ~1 Myr and 5 Myr. In contrast, paths 3, 4, and 5 spend more time at He partial-retention temperatures and therefore produce age-[eU] patterns that are more variable among the kinetics models (Fig. 3).

The versions of Path 5 tuned to three radiation damage accumulation and annealing models in the AHe system (Gautheron et al., 2009; Flowers et al., 2009; Willet et al., 2017) provide a particularly instructive result. The peak temperatures required by the Flowers- and Willet-tuned tT paths are within 0.5˚C of each other, meaning that they predict a 40 Ma age for a 60 μm and 60 ppm [eU] crystal with the effectively identical tT histories. Likewise, at [eU] < 40 ppm, the Willet- and Flowers-tuned paths predict very similar ages. However, these models diverge by >20 Myr at [eU] > 90 ppm; in other words, just because the Flowers- and Willet-tuned tT paths are identical does not mean they predict the same ages for all crystal compositions. In contrast, the version of Path 5 tuned to the Gautheron et al. (2009) kinetics model, which has a slightly higher peak temperature (Fig. 2), produces an age-[eU] trend that is similar to the Willet-tuned trend at [eU] > 60 ppm, similar to the Flowers- and Willet-tuned models at [eU] = 10 ppm, but different from both the Flowers- and Willet-tuned trends at [eU] = 30 ppm (Fig. 3). Thus, these simple forward models reveal the non-systematic differences among these kinetics models and in what types of thermal histories (i.e., paths 3, 4, and 5) these differences manifest most.

In this approach, it is critical to recognize that the largest differences in predicted He ages among kinetics models occurs for the [eU] values that are different from 60 ppm [eU] composition used to tune the paths, i.e., sometimes, but not always, the highest and lowest [eU] crystals in an age-[eU] pattern. This is a result inherent to the approach we have taken here: the tuning of the path to a fixed parameter (e.g., [eU] and grain size). The relative difference in cooling ages for each [eU] would be different for paths tuned to a 20 ppm crystal or a 100 ppm crystal. We emphasize that the choice of exactly how to tune a benchmark path depends on the application. Regardless of the details of how a path is tuned, it will always be the case that different kinetics models predict different patterns of data that depend on these parameters, and exploring the sensitivities of each parameter is important to understand in the modeling process.

For the ZHe system, the versions of Path 5 tuned to radiation damage accumulation and annealing models of Guenthner et al. (2013) and Ginster et al. (2019) have peak temperatures within 0.5°C of each other (Fig. 2), but the predicted age-[eU] distribution is also nearly identical. For these kinetics models, tuned Path 5 thermal histories predict cooling ages within ~ 1 Myr of each other for [eU] values ranging from 100 - 3000 ppm (Fig. 3).

This is also true for the other benchmark paths tuned to the Guenthner et al. (2013) and Ginster et al. (2019) kinetics models. This suggests that for 100-Myr-long thermal histories, the Guenthner and Ginster models will predict similar results. A third kinetics model—which for demonstration purposes simulates only damage accumulation, and not annealing (Guenthner, 2021)—has peak temperatures 1.5 - 2°C higher than models that incorporate annealing. This no-annealing model predicts an age-[eU] trend that only diverges from the others at [eU] > 600 ppm (Fig. 3), at crystal compositions where radiation damage accumulates more rapidly and thus the annealing of this damage is more impactful.

Finally, considering the track-length distributions for the AFT system is one way to explore

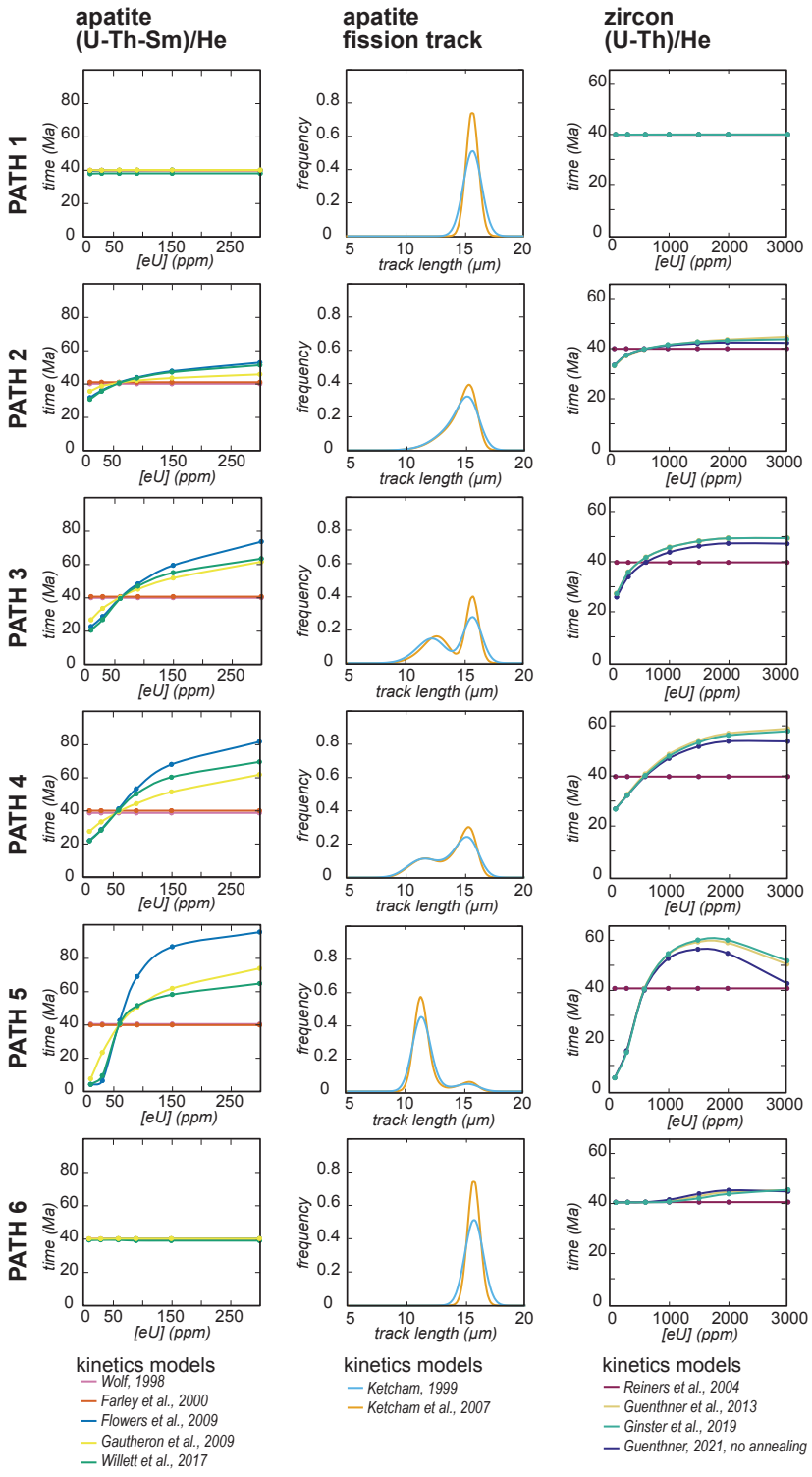

Figure 3. Expanding the data predicted by benchmark paths to include crystals with a range of grain [eU] compositions (AHe, ZHe) and track length distributions (AFT) shows data trends that can be used to distinguish among the predictions and interpretations of different kinetics models.

how different AFT kinetics models predict data distributions for crystals with the same chemistry (Fig. 3). Although benchmark paths for the Ketcham (1999) and Ketcham et al. (2007) kinetics models predict the same modalities and mean track lengths that vary by a maximum of ~0.15 μm, the uncertainties of mean track lengths can vary by as much as 0.25 μm. Consequently, the kinetics model of Ketcham et al. (2007) predicts a narrower peak(s) of track lengths for all Paths (Fig. 3). Versions of Path 5 tuned to each kinetics model produce identical mean track lengths, but uncertainty is 0.05 μm lower for track lengths predicted by the Ketcham et al. (2007) kinetics model. Interestingly, the uncertainty in mean track lengths, ~0.25 μm, is greatest for Paths 1 and 6 which have simple, fast cooling. This example uses track-length distributions, but modifying other parameters—for example, grain chemistry or its proxy, Dpar—could also be used to explore predictions from different AFT kinetics models.

6. A vision for the application of benchmark paths

Here, we demonstrate how a suite of benchmark tT paths can be designed to leverage the temperature sensitivity of a particular low-temperature thermochronometer (Fig. 1) and then tuned to specific kinetics models (Table 1, Fig. 2). We propose that the six benchmark paths we use in this work can provide a practical tool for the thermochronology community to use in a variety of contexts, including comparing kinetics models and predicting data patterns that arise from variable mineral compositions or geometries. This ‘design-then-tune’ approach is not meant to identify a single ‘best’ kinetics model for a particular system; instead, it is intended to quantify and visualize how kinetics models predict different tT conditions and data patterns. Having a common framework can also be used in the future to facilitate communicating how new kinetics models differ from existing models.

The design and tuning decisions we made here provide a common reference point for interpreting AHe, AFT, and ZHe data; however, a single suite of tuned paths cannot capture all complexities of these systems. For example, our proposed benchmark paths span a 100 Myr time frame (Fig. 1)—a time period that may be insufficient for capturing the accumulation of radiation damage and/or annealing that is a hallmark of the AHe and ZHe systems and is captured in those kinetics models. However, we note that our conceptual approach to benchmark path design could be applied to longer timescales. Despite the limitations of any one suite of benchmark paths, we envision that this approach can serve as an entry point to thinking critically about the relationship between the style of a tT history and the kinetic behaviors of chronometric systems that are sensitive to both temperature and time.

Acknowledgements
We thank two anonymous reviewers and the editorial staff at GChron for providing feedback on a version of this manuscript.
Competing Interests
None.
Author Contributions
ALSG, KEM, ALA, and MW all contributed to the project design and modeling. ALSG and KEM prepared the manuscript with contributions and revisions from all authors.

References

Carlson, W. D., Donelick, R. A., and Ketcham, R. A.: Variability of apatite fission-track annealing kinetics : I . Experimental results, Am. Mineral., 84, 1213–1223, 1999.

Donelick, R. A., Ketcham, R. A., and Carlson, W. D.: Variability of apatite fission-track annealing kinetics : II . Crystallographic orientation effects, Am. Mineral., 84, 1224–1234, 1999.

Farley, K. A.: Helium diffusion from apatite: General behavior as illustrated by Durango fluorapatite, J. Geophys. Res. Solid Earth, 105, 2903–2914, https://doi.org/10.1029/1999JB900348, 2000.

Flowers, R. M., Ketcham, R. A., Shuster, D. L., and Farley, K. A.: Apatite (U-Th)/He thermochronometry using a radiation damage accumulation and annealing model, Geochim. Cosmochim. Acta, 73, 2347–2365, https://doi.org/10.1016/j.gca.2009.01.015, 2009.

Gautheron, C., Tassan-Got, L., Barbarand, J., and Pagel, M.: Effect of alpha-damage annealing on apatite (U-Th)/He thermochronology, Chem. Geol., 266, 157–170, https://doi.org/10.1016/j.chemgeo.2009.06.001, 2009.

Ginster, U., Reiners, P. W., Nasdala, L., and Chanmuang N., C.: Annealing kinetics of radiation damage in zircon, Geochim. Cosmochim. Acta, 249, 225–246, https://doi.org/10.1016/j.gca.2019.01.033, 2019.

Guenthner, W. R.: Implementation of an Alpha Damage Annealing Model for Zircon (U-Th)/He Thermochronology With Comparison to a Zircon Fission Track Annealing Model, Geochemistry, Geophys. Geosystems, 22, 1–16, https://doi.org/10.1029/2019GC008757, 2021.

Guenthner, W. R., Reiners, P. W., Ketcham, R. A., Nasdala, L., and Giester, G.: Helium diffusion in natural zircon: radiation damage, anisotropy, and the interpretation of zircon (U-TH)/He thermochronology, Am. J. Sci., 313, 145–198, https://doi.org/10.2475/03.2013.01, 2013.

Ketcham, R. A., Donelick, R. A., and Carlson, W. D.: Variability of apatite fission-track annealing kinetics : III . Extrapolation to geological time scales, Am. Mineral., 84, 1235–1255, 1999.

Ketcham, R. A., Carter, A., Donelick, R. A., Barbarand, J., and Hurford, A. J.: Improved modeling of fission-track annealing in apatite, 92, 799–810, https://doi.org/10.2138/am.2007.2281, 2007.

Murray, K. E., Stevens Goddard, A. L., Abbey, A. L., and Wildman, M.: Thermal history modeling techniques and interpretation strategies: Applications using HeFTy, Geosphere, 18, 1622–1642, https://doi.org/10.1130/GES02500.1, 2022.

Reiners, P. W., Spell, T. L., Nicolescu, S., and Zanetti, K. A.: Zircon (U-Th)/He thermochronometry : He diffusion and comparisons with 40 Ar / 39 Ar dating, Geochim. Cosmochim. Acta, 68, 1857–1887, https://doi.org/10.1016/j.gca.2003.10.021, 2004.

Sobel, E. R. and Seward, D.: Influence of etching conditions on apatite fission-track etch pit diameter, Chem. Geol., 271, 59–69, https://doi.org/10.1016/j.chemgeo.2009.12.012, 2010.

Willett, C. D., Fox, M., and Shuster, D. L.: A helium-based model for the effects of radiation damage annealing on helium diffusion kinetics in apatite, Earth Planet. Sci. Lett., 477, 195–204, https://doi.org/10.1016/j.epsl.2017.07.047, 2017.

Wolf, R. A., Farley, K. A., and Silver, L. T.: Helium diffusion and low-temperature thermochronometry of apatite, Geochim. Cosmochim. Acta, 60, 4231–4240, https://doi.org/10.1016/S0016-7037(96)00192-5, 1996.

Wolf, R. A., Farley, K. A., and Kass, D. M.: Modeling of the temperature sensitivity of the apatite (U-Th)/He thermochronometer, Chem. Geol., 148, 105–114, https://doi.org/10.1016/S0009-2541(98)00024-2, 1998.